Structural Engineering and Mechanics, *Vol. 52, No. 4 (2014) 829-841*
DOI: http://dx.doi.org/10.12989/sem.2014.52.4.829

Theoretical analysis of overlay resisting crack propagation in old cement concrete pavement

Baofeng Pan[1], Yuanyuan Gao[*2] and Yang Zhong[1]

[1]*Faculty of Infrastructure Engineering, Dalian University of technology, Dalian Liaoning 116024, China*
[2]*College of Civil Engineering and Mechanics, Yan Shan University, Qinhuangdao Hebei 066004, China*

(Received February 5, 2013, Revised June 30, 2014, Accepted July 26, 2014)

Abstract. The main purpose of this study is to determine the effect of overlay on the crack propagation. In order to simplify the problem, a cement concrete pavement is modeled as an elastic plate on Winkler foundation. To derive the singular integral equations, the Fourier transform and dislocation density function are used. Lobatto-Chebyshev integration formula, as a numerical method, is used to solve the singular integral equations. The numerical solution of stress intensity factor at the crack tip is derived. In order to examine the effect of overlay for resisting crack propagation, numerical analyses are carried out for a cement concrete pavement with an embedded crack and a concrete pavement with an asphalt overlay. Results show the significant factors that influence the crack propagation.

Keywords: fourier transform; dislocation density function; singular integral equation; stress intensity factor; overlay

1. Introduction

Cement concrete pavement is a common structure of pavement. Since more and more cars and trucks are traveling on the road each day, damages in the form of cracks could be induced in the cement concrete pavement. Therefore, theoretical analysis of cement concrete pavement with embedded cracks or any other types of cracks is a significant and urgent research.

In 1950s, fracture mechanics was proposed as a discipline studying the strength of materials and structures containing cracks and it was a branch of solid mechanics (Ding 1997). Based on the fracture mechanics theory, complex function and integral transform are effective methods to solve these problems. For instance, Zak and William (1963) studied the stress intensity factor of two infinite planes with infinite crack and the crack terminated on the interface by using the complex function method. Erdogan and Gupta (1971) have obtained the analytic solution of composite materials containing crack in the interlayer by using integral transform. Integral transform was adopted by Sei and Tatsuya (2002) to solve the problem on multilayered composite with a crack perpendicular to the boundary and with the normal and symmetric uniform load distributed on the crack. However, complex function and integral transform methods can not solve problem in all conditions. Such as a perfect theory model for a cement concrete pavement with crack

∗Corresponding author, Ph.D., E-mail: gaoyuanyuan2286@163.com

http://www.techno-press.org/?journal=sem&subpage=8 ISSN: 1225-4568 (Print), 1598-6217 (Online)

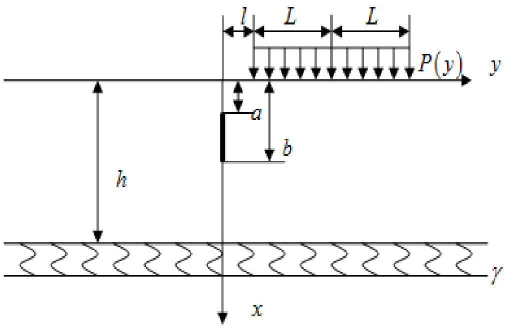

Fig. 1 Model of cement concrete pavement with a crack

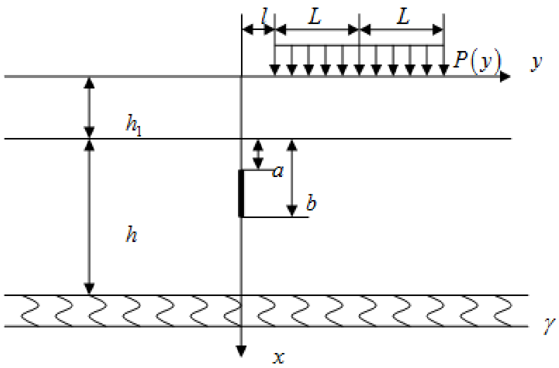

Fig. 2 Model of cement concrete pavement with an overlay containing a crack

perpendicular to the interface has not been built. At present, the pavement with a crack can be mostly analyzed by the finite element method (Long *et al*. 2008, Yang *et al*. 2009). Ghauch (2003) evaluated the response at the bottom of the hot-mix asphalt overlay on top of a concrete pavement. In order to identify the parameters involved in the deterioration of overlay, the effects of vehile speed, overlay thickness, and pavement temperature were investigated. Ameri *et al*. (2011) investigated an asphalt pavement containing a transverse top-down crack under traffic loading using 3D finite element analysis and the stress intensity factors were calculated for different distances between the crack and the vehicle wheels. Compared with the finite element method, the computational complexity and accuracy of the theoretical method is better.

In this paper, Fourier transform and dislocation density function are used to drive the singular integral equations. Lobatto-Chebyshev integration formula, as a numerical method, is used to solve the singular integral equations. The numerical results of stress anywhere of the plate and stress intensity factor at the crack tip are given. In order to examine the usefulness of the method, a cement concrete pavement with an embedded crack is considered. The results of the example are discussed and the factors that affect the stress and stress intensity factors are analyzed.

2. Description of the problem

The cement concrete pavement with a crack perpendicular to the interface is considered as a plate on an elastic foundation. Fig. 1 and Fig. 2 show the concrete pavement models without and with the overlay respectively. There is an embedded crack perpendicular to the boundaries of the plate as shown in the figures. In this study, only the plane strain is concerned, thus the effect of volume force is ignored. And the analytical solution for the model in Fig. 2, which is more complicated, is discussed in detail.

In order to simplify the problem shown in Fig. 2, based on the linear-elastic superposition principle, it is considered as three sub-problems, shown in Fig. 3, Fig. 4 and Fig. 5. The model of cement concrete pavement with an overlay containing a crack is equal to superposing the three sub-problems. The first part is simpler than the second one for obtaining the analytic solution and the formula deduction of third part is similar to the second one. Therefore, in this paper, the analytic solution of the second part is discussed mainly.

The boundary conditions of sub-problem 1 shown in Fig. 3

$$\sigma_{xx1}(0,y)=P(y), l<y<l+L; \sigma_{xy1}(0,y)=0, -\infty<y<\infty \tag{1}$$

$$\sigma_{xx2}(h_1+h,y)=\gamma u_2(h_1+h,y), \sigma_{xy2}(h_1+h,y)=0, -\infty<y<\infty \tag{2}$$

$$u_1(h_1,y)=u_2(h_1,y), v_1(h_1,y)=v_2(h_1,y), -\infty<y<\infty \tag{3}$$

$$\sigma_{xx1}(h_1,y)=\sigma_{xx2}(h_1,y), \sigma_{xy1}(h_1,y)=\sigma_{xy2}(h_1,y), -\infty<y<\infty \tag{4}$$

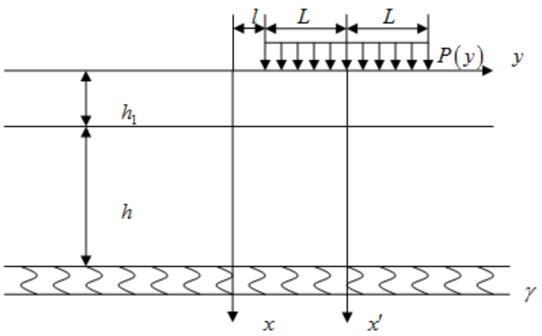

Fig. 3 Computational model of sub-problem 1

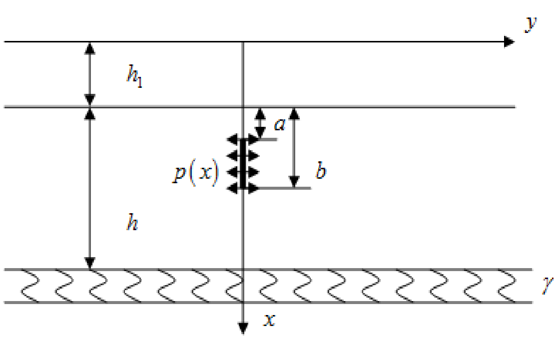

Fig. 4 Computational model of sub-problem 2

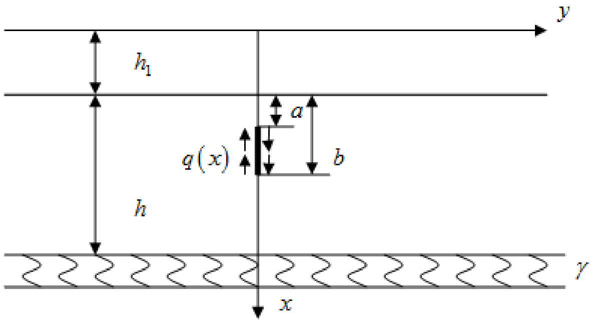

Fig. 5 Computational model of sub-problem 3

The boundary conditions of sub-problem 2 shown in Fig. 4

$$\sigma_{xx1}(0,y)=0,\sigma_{xy1}(0,y)=0,-\infty<y<\infty \tag{5}$$

$$\sigma_{xy1}(x,0)=0,v_1(x,0)=0,0<x<h_1 \tag{6}$$

$$\sigma_{xy2}(x,0)=0,h_1<x<h_1+h \tag{7}$$

$$v_2(x,0)=0,h_1<x<a+h_1 \ or \ b+h_1<x<h+h_1 \tag{8}$$

$$\sigma_{yy2}(x,0)=p(x),a+h_1<x<b+h_1 \tag{9}$$

$$\sigma_{xx2}(h_1+h,y)=\gamma u_2(h_1+h,y),\sigma_{xy2}(h_1+h,y)=0,-\infty<y<\infty \tag{10}$$

$$u_1(h_1,y)=u_2(h_1,y),v_1(h_1,y)=v_2(h_1,y),-\infty<y<\infty \tag{11}$$

$$\sigma_{xx1}(h_1,y)=\sigma_{xx2}(h_1,y),\sigma_{xy1}(h_1,y)=\sigma_{xy2}(h_1,y),-\infty<y<\infty \tag{12}$$

The boundary conditions of sub-problem 3 shown in Fig. 5

$$\sigma_{xx1}(0,y)=0,\sigma_{xy1}(0,y)=0,-\infty<y<\infty \tag{13}$$

$$\sigma_{yy1}(x,0)=0,u_1(x,0)=0,0<x<h_1 \tag{14}$$

$$\sigma_{yy2}(x,0)=0,h_1<x<h_1+h \tag{15}$$

$$u_2(x,0)=0,h_1<x<a+h_1 \ or \ b+h_1<x<h+h_1 \tag{16}$$

$$\sigma_{xy2}(x,0)=q(x),a+h_1<x<b+h_1 \tag{17}$$

$$\sigma_{xx2}(h_1+h,y)=\gamma u_2(h_1+h,y),\sigma_{xy2}(h_1+h,y)=0,-\infty<y<\infty \tag{18}$$

$$u_1(h_1,y)=u_2(h_1,y),v_1(h_1,y)=v_2(h_1,y),-\infty<y<\infty \tag{19}$$

$$\sigma_{xx1}(h_1,y)=\sigma_{xx2}(h_1,y),\sigma_{xy1}(h_1,y)=\sigma_{xy2}(h_1,y),-\infty<y<\infty \tag{20}$$

Where σ_{xxn} and σ_{yyn} are the x and y components of the stress vector in the n layer, respectively. σ_{xyn} is the shearing stress in the n layer. u_n and v_n are the x and y components of the displacement vector in the n layer, respectively. n=1,2. γ is the stiffness of the foundation.

3. Solution of *p*(*x*) and *q*(*x*)

In sub-problem 1, in order to simplify this problem, coordinate translation method is adopted. The y coordinate axis is moved "$l+L$" units to right, the model is reduced from a plane strain problem with Asymmetric load vertical to the boundary to symmetric load. In terms of theory of linear-elastic superposition, $p(x)$ and $q(x)$ in sub-problem 2 and sub-problem 3 can be expressed in the following forms

$$p(x)=-\sigma_{yy}(x,-l-L);q(x)=-\sigma_{xy}(x,-l-L) \tag{21}$$

4. Theoretical analysis of sub-problem 2

The governing equations of plane elasticity may be expressed as (Li 2000)

$$(1+k)\frac{\partial^2 u}{\partial x^2}+(3-k)\frac{\partial^2 v}{\partial x\partial y}+(k-1)(\frac{\partial^2 u}{\partial y^2}+\frac{\partial^2 v}{\partial x\partial y})=0 \tag{22}$$

$$(3-k)\frac{\partial^2 u}{\partial x\partial y}+(1+k)\frac{\partial^2 v}{\partial y^2}+(k-1)(\frac{\partial^2 v}{\partial x^2}+\frac{\partial^2 u}{\partial x\partial y})=0 \tag{23}$$

where k=(3−v)/(1+v) for plane stress, k=3−v for plane strain and u, v are the x, y components of the displacement vector, respectively. v is Poisson's ratio. In this paper, k=3−4v is selected corresponding to the case of plane strain.

From Hooke's Law, the stress components can be expressed as

$$\begin{aligned}\sigma_{xx}&=\frac{G}{k-1}[(1+k)\frac{\partial u}{\partial x}+(3-k)\frac{\partial v}{\partial y}]\\ \sigma_{yy}&=\frac{G}{k-1}[(3-k)\frac{\partial u}{\partial x}+(1+k)\frac{\partial v}{\partial y}]\\ \sigma_{xy}&=G(\frac{\partial u}{\partial y}+\frac{\partial v}{\partial x})\end{aligned} \tag{24}$$

where G is the shear modulus of the material.

In order to achieve the solutions of the displacement components, the displacement u_n and v_n in the n layer can be expressed with Fourier integral formulas (Zhao 1998)

$$u_n(x,y)=\frac{2}{\pi}\int_0^{\infty} f_{n1}(x,\eta)\cos(\eta y)\,d\eta+\frac{1}{2\pi}\int_{-\infty}^{\infty} g_{n1}(\xi,y)e^{i\xi x}d\xi \tag{25}$$

$$v_n(x,y)=\frac{2}{\pi}\int_0^{\infty} f_{n2}(x,\eta)\sin(\eta y)\,d\eta+\frac{1}{2\pi}\int_{-\infty}^{\infty} g_{n2}(\xi,y)e^{i\xi x}d\xi \tag{26}$$

Substituting Eqs. (25) and (26) into Eqs. (22) and (23), one can obtain the expressions of displacements u_n and v_n.

$$u_n(x,y)=\frac{2}{\pi}\int_0^{\infty}[e^{\eta x}(A_{n1}+A_{n2}x)+e^{-\eta x}(A_{n3}+A_{n4}x)]\cos(\eta y)\,d\eta+\frac{1}{2\pi}\int_{-\infty}^{\infty} e^{i\xi x-|\xi|y}(B_{n3}+B_{n4}y)d\xi \tag{27}$$

$$\begin{aligned}v_n(x,y)=\frac{2}{\pi}\int_0^{\infty}\frac{1}{\eta}\{-e^{\eta x}[\eta A_{n1}+(\eta x+k)]A_{n2}+e^{-\eta x}\\ [\eta A_{n3}+(\eta x-k)A_{n4}]\}\sin(\eta y)d\eta+\frac{1}{2\pi}\int_{-\infty}^{\infty}\frac{ie^{i\xi x-|\xi|y}}{\xi}[|\xi|B_{n3}+(k+|\xi|y)B_{n4}]d\xi\end{aligned} \tag{28}$$

where B_{n3} and B_{n4} are the functions of ξ and A_{n1}, A_{n2}, A_{n3} and A_{n4} are the functions of η.

Substituting Eqs. (27) and (28) into Eq. (24), the components of stress are given by

$$\begin{aligned}\sigma_{xxn}=\frac{2G_n}{\pi}\int_0^{\infty}\{e^{\eta x}[2\eta A_{n1}+(k-1+2\eta x)A_{n2}]+e^{-\eta x}[-2\eta A_{n3}+(k-1-2\eta x)A_{n4}]\}\\ \cos(\eta y)d\eta+\frac{\mu}{2\pi}\int_{-\infty}^{\infty}\frac{ie^{i\xi x-|\xi|y}}{\xi}\left[2(k-1)\xi^2(B_{n3}+B_{n4}y)+|\xi|(k^2-4k+3)B_{n4}\right]d\xi\end{aligned} \tag{29}$$

$$\begin{aligned}\sigma_{yyn}=\frac{2G_n}{\pi}\int_0^{\infty}\{e^{\eta x}[-2\eta A_{n1}-(k+3+2\eta x)A_{n2}]+e^{-\eta x}[2\eta A_{n3}-(k+3-2\eta x)A_{n4}]\}\\ \cos(\eta y)d\eta+\frac{\mu}{2\pi}\int_{-\infty}^{\infty}\frac{ie^{i\xi x-|\xi|y}}{\xi}\left[2(k-1)\xi^2B_{n3}+2(1-k)\xi^2yB_{n4}+(1-k^2)|\xi|B_{n4}\right]d\xi\end{aligned} \tag{30}$$

$$\begin{aligned}\sigma_{xyn}=\frac{2G_n}{\pi}\int_0^{\infty}\{e^{\eta x}[-2\eta A_{n1}-(k+1+2\eta x)A_{n2}]+e^{-\eta x}[-2\eta A_{n3}+(k+1-2\eta x)A_{n4}]\}\\ \sin(\eta y)d\eta-\frac{\mu}{2\pi}\int_{-\infty}^{\infty}e^{i\xi x-|\xi|y}\left[(k-1)B_{n4}+2|\xi|(B_{n3}+B_{n4}y)\right]d\xi\end{aligned} \tag{31}$$

For convenience, dislocation density function is introduced, which is defined as (Zhao 1998)

$$\phi(x)=\frac{\partial v(x,0)}{\partial x};\quad \phi(x)=0,\quad 0<x<a \text{ or } b<x<h;\quad \int_a^b\phi(x)dx=0。$$

Based on Eqs. (6) and (7) and the theory of residue, B_{13}, B_{14}, B_{23} and B_{24} are expressed respectively as

$$B_{13}=0, B_{14}=0, B_{23}=\int_a^b\frac{(k-1)e^{i\xi x}}{(k+1)|\xi|}\phi(t)\,dt, B_{24}=\int_a^b\frac{-2e^{i\xi x}}{(k+1)}\phi(t)\,dt \tag{32}$$

while the boundary conditions (5), (10)-(12) are expressed as the following in terms of inverse Fourier transform and residue theorem

$$2\eta A_{11} + \left(k-1\right)A_{12} - 2\eta A_{13} + \left(k-1\right)A_{14} = 0 \tag{33}$$

$$-2\eta A_{11} - \left(k+1\right)A_{12} - 2\eta A_{13} + \left(k+1\right)A_{14} = 0 \tag{34}$$

$$\begin{aligned} &e^{\eta\left(h+h_1\right)}\{(2\eta\beta-1)A_{21} + [\beta(k-1+2\eta h+2\eta h_1)-(h+h_1)]A_{22}\} \\ &+e^{-\eta\left(h+h_1\right)}\{(-2\eta\beta-1)A_{23} + [\beta(k-1-2\eta h-2\eta h_1)-(h+h_1)]A_{24}\} = \int_{a+h_1}^{b+h_1} F_1\left(\eta,t\right) f_1\left(t\right)dt \end{aligned} \tag{35}$$

$$\begin{aligned} &e^{\eta h_2}[-2\eta A_{21} - \left(k+1+2\eta h_1+2\eta h\right)A_{22}] + e^{-\eta h_2}[-2\eta A_{23} + (k+1-2\eta h_1-2\eta h)A_{24}] \\ &= \int_{a+h_1}^{b+h_1} F_2\left(\eta,t\right) f_1\left(t\right)dt \end{aligned} \tag{36}$$

$$\begin{aligned} &e^{\eta h_1}\left(A_{11}+A_{12}h_1\right) + e^{-\eta h_1}\left(A_{13}+A_{14}h_1\right) \\ &-e^{\eta h_1}\left(A_{21}+A_{22}h_1\right) - e^{-\eta h_1}\left(A_{23}+A_{24}h_1\right) = \int_{a+h_1}^{b+h_1} F_3\left(\eta,t\right) f_1\left(t\right)dt \end{aligned} \tag{37}$$

$$\begin{aligned} &\frac{1}{\eta}\{-e^{\eta h_1}[\eta A_{11} + \left(\eta h_1 + k\right)A_{12}] + e^{-\eta h_1}[\eta A_{13} + \left(\eta h_1 - k\right)A_{14}]\} \\ &-\frac{1}{\eta}\{-e^{\eta h_1}[\eta A_{21} + \left(\eta h_1 + k\right)A_{22}] + e^{-\eta h_1}[\eta A_{23} + \left(\eta h_1 - k\right)A_{24}]\} \\ &= \int_{a+h_1}^{b+h_1} F_4\left(\eta,t\right) f_1\left(t\right)dt \end{aligned} \tag{38}$$

$$\begin{aligned} &\alpha\{e^{\eta h_1}[2\eta A_{11} + \left(k-1+2\eta h_1\right)A_{12}] + e^{-\eta h_1}[-2\eta A_{13} + \left(k-1-2\eta h_1\right)A_{14}]\} \\ &-\{e^{\eta h_1}[2\eta A_{21} + \left(k-1+2\eta h_1\right)A_{22}] + e^{-\eta h_1}[-2\eta A_{23} + \left(k-1-2\eta h_1\right)A_{24}]\} \\ &= \int_{a+h_1}^{b+h_1} F_5\left(\eta,t\right) f_1\left(t\right)dt \end{aligned} \tag{39}$$

$$\begin{aligned} &\alpha\{e^{\eta h_1}[-2\eta A_{11} - \left(k+1+2\eta h_1\right)A_{12}] + e^{-\eta h_1}[-2\eta A_{13} + \left(k+1-2\eta h_1\right)A_{14}]\} \\ &-\{e^{\eta h_1}[-2\eta A_{21} - \left(k+1+2\eta h_1\right)A_{22}] + e^{-\eta h_1}[-2\eta A_{23} + \left(k+1-2\eta h_1\right)A_{24}]\} \\ &= \int_{a+h_1}^{b+h_1} F_6\left(\eta,t\right) f_1\left(t\right)dt \end{aligned} \tag{40}$$

where $\alpha = \frac{G_1}{G_2}$ and $\beta = \frac{G_2}{\gamma}$. G_1 is the shear modulus of the material in the first layer, G_2 is the shear modulus of the material in the second layer.

$$F_1\left(\eta,t\right) = \frac{e^{\eta(t-h_1-h)}\{8\beta\eta^2(h_1+h-t)+[2(k-1)+4\eta(h_1+h-t)]\}}{4\eta(k+1)};$$

$$F_2(\eta,t)=\frac{2e^{\eta(t-h_1-h)}[\eta(h_1+h-t)-1]}{(k+1)};\quad F_3(\eta,t)=\frac{(k-1)e^{\eta(t-h_1)}}{2\eta(k+1)}+\frac{(h_1-t)e^{\eta(t-h_1)}}{(k+1)};$$

$$F_4(\eta,t)=\frac{1}{2}\left(\frac{e^{\eta(t-h_1)}}{\eta}-1\right)-\frac{(h_1-t)e^{\eta(t-h_1)}}{(k+1)};\quad F_5(\eta,t)=-\frac{2\eta(h_1-t)e^{\eta(t-h_1)}}{(k+1)};$$

$$F_6(\eta,t)=-\frac{2\left[\eta(h_1-t)-1\right]e^{\eta(t-h_1)}}{(k+1)}$$

Solving Eqs. (33)-(40) for A_{11}, A_{12}, A_{13}, A_{14}, A_{21}, A_{22}, A_{23} and A_{24} in terms of $\phi(t)$ and substituting A_{21}, A_{22}, A_{23}, A_{24}, B_{23} and B_{24} into the boundary condition Eq. (9), it yields

$$\int_a^b K_1(x,t)\phi(t)\,dt+\int_a^b K_2(x,t)\phi(t)\,dt=\frac{(k+1)\pi}{4G_2}p(x) \tag{41}$$

where $K_1(x,t)=\int_{-\infty}^{\infty}\frac{1}{2}\left(\frac{i\xi}{|\xi|}\right)e^{i\xi(x-t)}d\xi$. With the assistance of the result $i\int_{-\infty}^{\infty}\operatorname{sgn}(\xi)e^{i\xi(x-t)}d\xi=-\frac{2}{x-t}$, one can obtain: $K_1(x,t)=\frac{1}{t-x}$. $\varphi(x,t,\eta)$ and $p(x)$ can be solved by Gauss-Laguerre quadrature.

To solve the integral equation numerically by using a collocation technique, the interval (a, b) in Eq. (41) is normalized and expressed as

$$\int_{-1}^{1}\frac{g(r)}{r-s}dr+\int_{-1}^{1}K(s,r)\,g(r)dr=\frac{(k+1)\pi}{4G}f(s) \tag{42}$$

For an embedded crack, the solution of the integral Eq. (42) can be expressed as: $g(r)=F(r)\big/\sqrt{1-r^2}$.

Lobatto-Chebyshev integration formula is then used to solve the singular integral equations. The singular integral equation is converted to a system of linear equations by means of this numerical method. The expression of Eq. (42) can be written as

$$\sum_{j=1}^{n}\omega_j F(r_j)[\frac{1}{r_j-s_i}+K(r_j,s_i)]=\frac{(k+1)\pi}{4\mu}f(s_i) \tag{43}$$

In Eq. (43), there are n-1 equations and the last equation comes from the property of dislocation density function which is expressed as $\int_{-1}^{1}\mathrm{g}(\mathrm{r})\mathrm{dr}=0$ for the embedded crack. It is also written as

$$\sum_{j=1}^{n}\omega_j F(r_j)=0 \tag{44}$$

where ω_j is the weight function $\omega_j=\pi/(n-1)$, $j=2,\ldots,n-1$, $\omega_1=\omega_1=\pi/2(n-1)$; $r_j=\cos((j-1)\pi/(n-1))$, $j=1,\ldots,n$; $s_i=\cos((2i-1)\pi/(2n-1))$, $i=1,\ldots,n-1$.

The stress intensity factors are defined and evaluated as (Kadioğlu *et al*. 1998)

$$K_{Ia} = \lim_{x\to a}\sqrt{2(a-x)}\sigma_{yy2}\left(x,0\right), K_{Ib} = \lim_{x\to b}\sqrt{2(x-b)}\sigma_{yy2}\left(x,0\right) \tag{45}$$

Substituting the numerical solution into Eq. (45), one can obtain

$$K_{Ia} = -4\mu/(k+1)\sqrt{b-a/2}F\left(-1\right), K_{Ib} = 4\mu/(k+1)\sqrt{b-a/2}F\left(1\right) \tag{46}$$

Substituting A_{11}, A_{12}, A_{13}, A_{14}, A_{21}, A_{22}, A_{23}, A_{24}, B_{13}, B_{14}, B_{23} and B_{24} into Eqs. (27)-(31), stress and displacement at any positions shown in Fig. 4 can be derived. The same method can also be used to solve the model shown in Fig. 5.

5. Numerical examples and discussion

In order to verify the achieved formulation and compare the stress intensity factors of model 1 (as shown in Fig. 1) and model 2 (as shown in Fig. 2). The parameters for the model 1 are: P=700000 N/m, L=0.15 m, E=3.1×1010 N/m^2, G=1.1482×1010 Mpa, γ=1.3×109 N/m^3, h=0.25 m, ν=0.35. In the case of plane strain problem, k=1.6, β=G/γ=8.832, length of crack d=b-a. The parameters for the model 2 are: P=700000 N/m, L=0.15 m, E_1=4.32×109 N/m^2, G_1=1.6×109 N/m^2, h_1=0.1 m, ν_1=0.35, k_1=1.6, E_2=3.1×1010 N/m^2, G_2=1.1482×1010 N/m^2, γ=1.3×109 N/m^3, h_2=0.25 m, ν_2=0.35, k_2=1.6, β=G_2/γ=8.832.

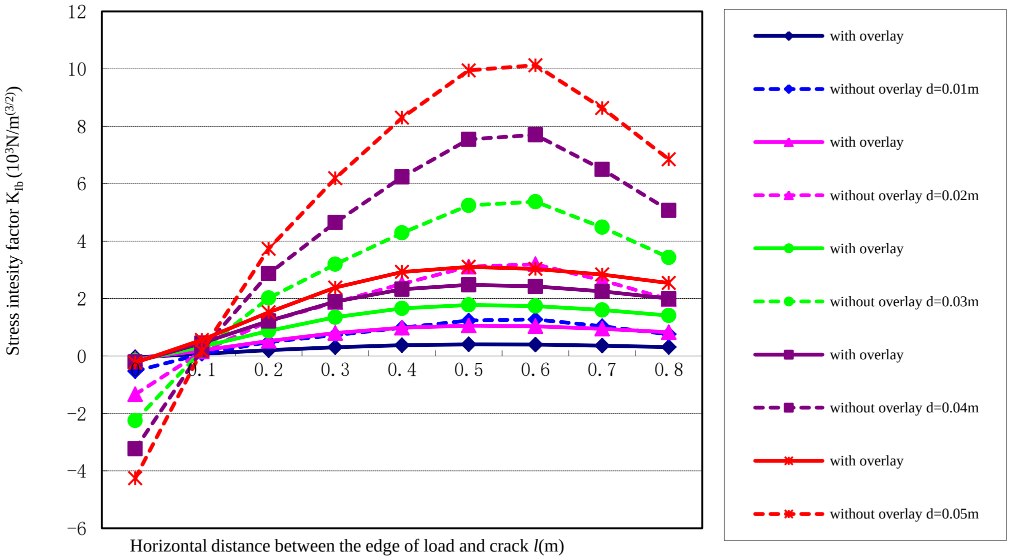

Fig. 6 Comparison of stress intensity factors K_{Ib} of the crack tip (b) with and without overlay on old cement concrete pavement (old cement concrete pavement containing perpendicular crack)

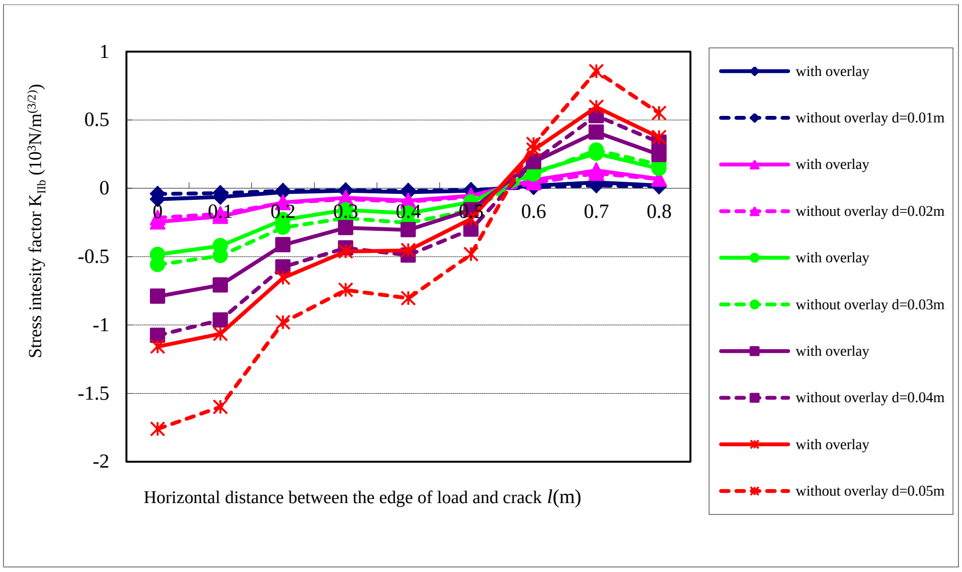

Fig. 7 Comparison of stress intensity factors $K_{IIb}$of the crack tip (b) with and without overlay on old cement concrete pavement (old cement concrete pavement containing perpendicular crack)

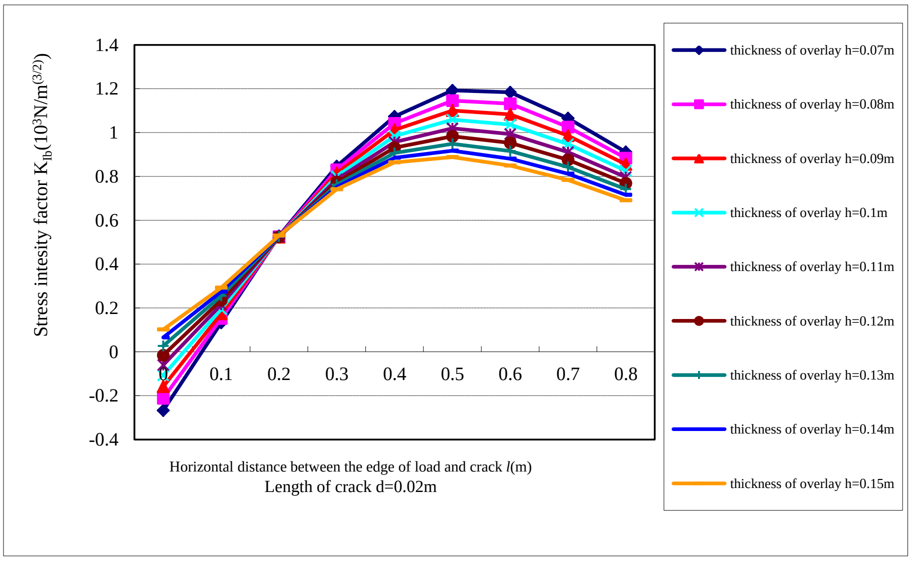

Fig. 8 Result of stress intensity factor K_{Ib} of the crack tips (b) with different thickness (thickness from 7 cm to 15 cm) of overlay on old cement concrete pavement (old cement concrete pavement containing perpendicular crack)

For comparing the old cement concrete pavement with and without asphalt overlay, the stress intensity factors of the crack tips are calculated for model 1 and model 2, and the results are shown in Figs. 6 and 7. As the thickness of the overlay and the shear modulus of the material are important factors which affect the stress intensity factors, the results calculated with different thickness and shear modulus are shown in Figs. 8-11.

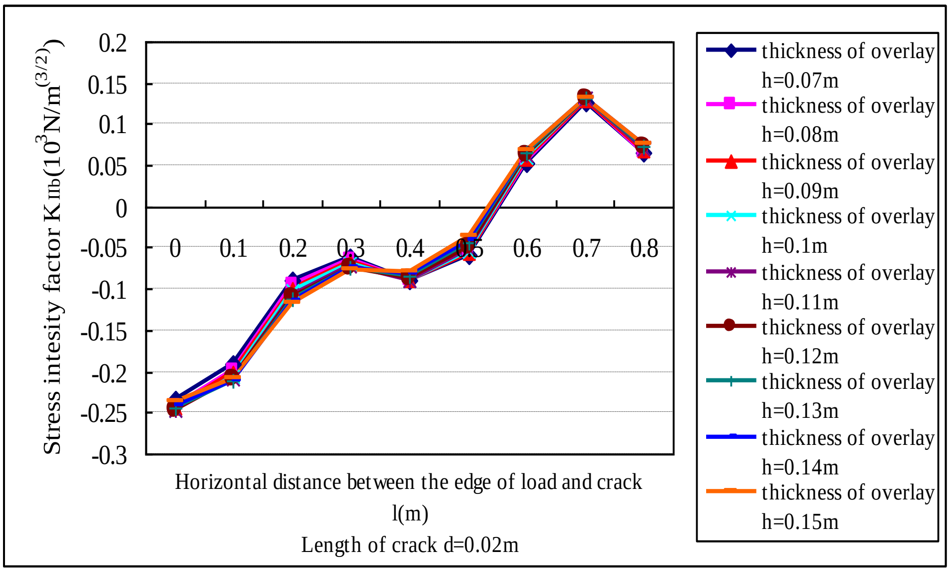

Fig. 9 Result of stress intensity factor K_{IIb} of the crack tips (b) with different thickness (thickness from 7 cm to 15 cm) of overlay on old cement concrete pavement (old cement concrete pavement containing perpendicular crack)

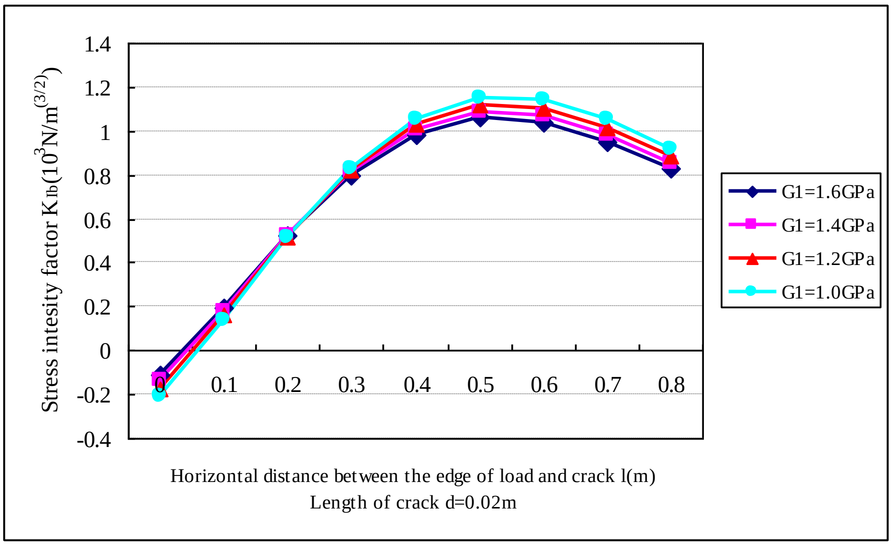

Fig. 10 Result of stress intensity factor K_{Ib} of the crack tips (b) with different shear modulus shear modulus from 1.0 GPa to 1.6 GPa) of overlay on old cement concrete pavement (old cement concrete pavement containing perpendicular crack) horizontal distance between the edge of load and crack

The effect of asphalt overlay is investigated by comparing the values of stress intensity factors of crack tip in pavement with and without an 10cm thickness overlay, while keeping all other parameters fixed. Fig. 6 and Fig. 7 show, no matter I type crack or II type crack, the stress intensity factors of the crack tips (b) in the pavement with overlay are smaller than that in pavement without

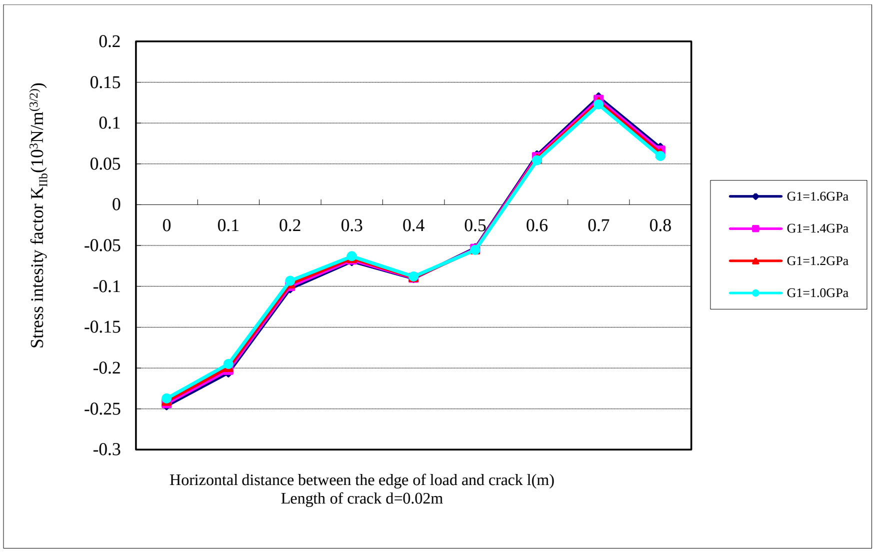

Fig. 11 Result of stress intensity factor K_{IIb} of the crack tips (b) with different shear modulus (shear modulus from 1.0GPa to 1.6GPa) of overlay on old cement concrete pavement (old cement concrete pavement containing perpendicular crack)

overlay. Furthermore, the stress intensity factors of I type crack decrease dramatically. The values of stress intensity factors of I type crack tips (b) in the pavement with overlay are reduced to approximate 50% of without overlay, with the same load position and identical crack length. It indicates that using the overlay is an effective way for lowering the crack extension.

The effect of overlay thickness is examined using different overlay thickness, with all other parameters fixed. Fig. 8 and Fig. 9 show, with the thickness of the overlay increasing from 7 cm to 15 cm, the stress intensity factors of I type crack decrease slightly, while the stress intensity factors of II type crack do not presence obvious change. Therefore, it is not wise choice to increase the thickness of overly directly. Grid or other Geosynthetic could be considered as a Interlayer to reinforce on mitigating reflection cracking in asphalt overlays and theoretical analysis of these structure will be conducted in the later research.

The effect of shear modulus of overlay is also examined. From the 4 overlapping curves almost in Fig. 11, with the increasing of shear modulus of overlay from 1.0 GPa to 1.6 GPa, the stress intensity factors of II type crack have not change. In Fig. 10, stress intensity factors of I type crack are decreased slightly as the shear modulus of overlay increase, while the horizontal distance between the edge of load and crack exceed 0.25m. It denotes that the shear modulus of overlay is not a significant factor that influences the crack propagation in old cement concrete pavement and it is not appropriate method to improve the effect of overlaying by changing the overly modulus.

6. Conclusions

Based on the theory of fracture mechanics, the method of Fourier transform and dislocation density function in association with solving the singular integral equations are introduced to calculate the stress and stress intensity factors in a cement concrete pavement which contains a crack perpendicular to the interface and with asphalt overlay on it. This method can be used to analyze effect of asphalt overlay for resisting crack propagation. Current numerical simulation indicates that the asphalt overlay on top of the old concrete pavement plays an important role for protecting the structure from the crack damage. The thickness and the shear modulus of the overlay are not the two significant factors that affect the overlay.

Acknowledgements

The authors gratefully acknowledge the support from the National Natural Science Foundation of China (Grant 51178085).

References

Ameria, M., Mansourian, A., Khavas, M.H. *et al*. (2011), “Ayatollahi cracked asphalt pavement under traffic loading-a 3D finiteelement analysis”, *Eng. Fract. Mech.*, **78**, 1817-1826.

Ding, S.D. (1997), *Fracture Mechanics*, China Machine Press, Beijing, China.

Erdogan, F. and Gupta, G. (1971), “The stress analysis of multi-layered composites with a flaw”, *Int. J. Solid. Struct.*, **7**, 39-61.

Ghauch, Z.G. and Abou-Jaoude, G.G. (2003), “Strain response of hot-mix asphalt overlays in jointed plain concrete pavements due to reflective cracking”, *Comput. Struct.*, **124**, 38-46.

Kadioğlu, S., Dağ, S. and Yahsi, S. (1998), “Crack problem for a functionally graded layer on an elastic foundation”, *Int. J. Fract.*, **94**, 63-77.

Li, Y.D. (2000), *Theory and Application of Fracture Mechanics*, Science press, Beijing, China.

Long, G., Wang, C.H. and Liu, J.R. (2008), “Three-dimensional numerical analysis for reflective crack of asphalt pavement”, *Highw. Eng.*, **33**(2), 139-142.

Sei, U. and Tatsuya, M. (2002), “The surface crack problem for layered elastic medium with a functionally graded non-homogeneous interface”, *J. Solid Mech. Mater. Eng.*, **45**(3), 371-378.

Yang, D.C., Zhao, W.T. and Li, L.J. (2009), “Analysis of reflection cracks of asphalt concrete overlay over used cement concrete pavements by finite element analysis”, *Huazhong Univ. Sci. Tech. (Natural Science Edition)*, **37**(1), 61-64.

Zak, A.R. and Williams, M.L. (1963), “Crack point stress singularities at a bi-material interface”, *J. Appl. Mech.*, **30**, 142-143.

Zhao, H.Q. (1998), “Fracture and fatigue analysis of functionally graded and homogeneous materials using singular integral equation approach”, Ph.D. Dissertation, Baltimore, Johns Hopkins University.

CC